

Calibration of stiffness and strength for layered rocks

Kaimin Yue, Jon E. Olson, and Richard A. Schultz

Petroleum and Geosystems Engineering, The University of Texas at Austin, Austin, TX, USA

Copyright 2016 ARMA, American Rock Mechanics Association

This paper was prepared for presentation at the 50th US Rock Mechanics / Geomechanics Symposium held in Houston, TX, USA, 26 June-29 June 2016.

This paper was selected for presentation at the symposium by an ARMA Technical Program Committee based on a technical and critical review of the paper by a minimum of two technical reviewers. The material, as presented, does not necessarily reflect any position of ARMA, its officers, or members. Electronic reproduction, distribution, or storage of any part of this paper for commercial purposes without the written consent of ARMA is prohibited. Permission to reproduce in print is restricted to an abstract of not more than 200 words; illustrations may not be copied. The abstract must contain conspicuous acknowledgement of where and by whom the paper was presented.

ABSTRACT: Oil and gas production from unconventional reservoirs requires drilling and hydraulic fracturing within a layered reservoir, which is usually stratified with a variety of stiff and soft layers. The overall strength of layered rocks is useful for predicting their stability or failure under production conditions, which may contribute to vertical height containment of hydraulic fractures in an unconventional reservoir. In this work, triaxial experimental testing of reservoir-analog materials and three-dimensional Particle Flow Code (PFC3D) simulations were used to evaluate the contributions of layer properties, such as number, thickness, and sequence, on the average strength of a layered reservoir.

The laboratory and PFC simulation results show that the stiffness and strength of a layered sequence are not affected by factors such as bedding plane strength, the number of layers, or layer thickness. However its stiffness and strength can be related to the relative proportions of stiff and soft layers. The stiffness of the layered sequences obtained from the experiments and PFC models are closely predicted by a calculated harmonic average stiffness of the sequence. The stiffness-strength relation obtained from the reservoir-analog materials has a similar form to those in the literature that were obtained from natural rock types, supporting the utility of PFC models of layered sequences. These results support the use of harmonic average and PFC simulations in estimating elastic stiffness and strength in layered and unconventional reservoir sequences.

1. INTRODUCTION

Oil and gas production from unconventional reservoirs generally requires hydraulic fracturing within a layered reservoir, which is usually stratified with layers of different mechanical properties. For instance, Eagle Ford shale is a well laminated reservoir with alternating stiff carbonate rich layers and soft clay rich layers [1]. In order to produce hydrocarbon from unconventional reservoirs more efficiently and economically, a better understanding of hydraulic fracture propagation in layered reservoirs is needed. Among all the issues, vertical height growth of hydraulic fractures is recognized as one of the critical factors to the success of hydraulic fracturing treatments [2, 3]. If the expected hydraulic height growth is not achieved, a large area of payzone will not be stimulated which affects the production. In contrast, if hydraulic fractures grow into the adjacent rock layers which are not productive, an excessive amount of injection fluid and proppants will be wasted [4].

Given its importance, hydraulic fracture propagation in the vertical direction and height containment have been extensively studied by numerical modeling [3, 5, 6], mineback tests [7], and laboratory testing [8]. The results indicate that fracture geometry is complex and fracture height is mainly affected by the heterogeneities of both

stress and mechanical properties, as well as the interface properties of bedding planes.

Cost-effective hydraulic fracturing design requires fractures to access as much reservoir payzone as possible. The critical issue is to understand and predict how hydraulic fractures can be contained to the interval of interest. As shown in the extensive fracture mapping database [2], hydraulic fractures are often better contained vertically than that is predicted by models or conventional wisdom. Micro-seismic data and micro-deformation data show that fracture length can sometimes exceed 300 meters (around 1000 feet), whereas fracture height is much smaller, usually measured in tens of meters [2].

Additionally, hydraulic fractures in some shale plays such as Eagle Ford shale, Woodford shale, and Barnett shale exhibit little out-of-zone height growth and are usually well contained within the same rock stack which contains multiple rock layers [2]. However, in other relatively continuous shales such as Marcellus shale and Haynesville shale, fracture growth into the adjacent rock stacks is often observed and height containment is usually poor [9]. As a result, compared to the mechanical properties of rock layers, the overall mechanical properties of stratified rock stack might be

more important to evaluate hydraulic fracture height containment in layered reservoirs.

In this study, triaxial experimental testing of reservoir-analog materials and Particle Flow Code (PFC) [10] simulations were used to evaluate the contributions of layer properties, such as number, thickness, and strength, on the average strength of a layered reservoir, which may contribute to vertical height containment of hydraulic fractures in an unconventional reservoir. The harmonic Young's modulus of stratified layer stack is defined, which is also important for fracture height containment due to stiffness contrast between adjacent layer stacks.

2. EXPERIMENTAL SETUP

The experimental apparatus used in the triaxial testing is shown schematically in Fig. 1. It contains three parts: a loading frame, a pump, and an aluminum confining vessel. The HUMBOLDT loading frame provides an axial load and the pump applies confining pressure on a cylindrical sample. The aluminum confining vessel can hold a 25.4-mm (1-inch) diameter and 50.8-mm (2-inch) long cylindrical sample.



Fig. 1. Illustration of experimental apparatus.

In order to evaluate the mechanical behavior of stiff/soft layered samples, two kinds of synthetic rocks are used to mimic the behavior of stiff and soft rocks in our experiments, respectively. In the experiments, synthetic hydrostone is used as stiff rocks and sand is used to mimic the behavior of soft rocks. Synthetic hydrostone is composed of gypsum and cement, and is produced by United States Gypsum Company (IG-123-F1-50BAG/6-99). Table 1 shows the ratio of water and dry cement by weight for hydrostone [11]. Well-mixed liquefied hydrostone is first poured to a 25.4-mm diameter mold and then kept at room temperature for at least three days to make sure it is perfectly solid.

Table 1. Mixing percentage for hydrostone [11]

Material	Dry cement weight	Water weight
Hydrostone	75.7 %	24.3 %

The mechanical properties of hydrostone are determined by triaxial experiments with various confining stresses. Based on the peak load at different confining pressures, the Mohr-Coulomb criterion can be used to calculate the unconfined compressive stress and the friction coefficient.

$$\sigma_1 = n\sigma_3 + UCS \quad (1)$$

$$\mu_i = \frac{n-1}{2\sqrt{n}} \quad (2)$$

where σ_1 is the peak axial stress, σ_3 is the confining stress, UCS is the unconfined compressive stress, n is the slope of the σ_3 vs. σ_1 curve, which is related to the internal friction coefficient, μ_i . For hydrostone, the unconfined compressive stress is measured as 40.2 MPa and the friction coefficient is determined as 0.56. By matching the slope of the linear portion of the axial stress-strain curve, Young's modulus is determined to be around 6.2 GPa. Following the same procedure, the friction coefficient and Young's modulus of sand are determined as 0.79 and 363 MPa, respectively.

In order to evaluate the layering effect on the mechanical properties of stiff/soft layered rocks, two kinds of synthetic samples (Fig. 2) are utilized in the triaxial experiments. These two samples contain the same volume fraction of hydrostone (stiff material) and sand (soft material). However, they have different layer thicknesses. The first sample has two layers with one hydrostone layer (25.4 mm) and one sand layer (25.4 mm). The second sample has four layers with two hydrostone layers (12.7 mm) and two sand layers (12.7 mm). Based on the triaxial testing under different confining stresses, the unconfined compressive stress of two layered sample and four layered sample are measured to be 3.0 MPa and 8.9 MPa, respectively.

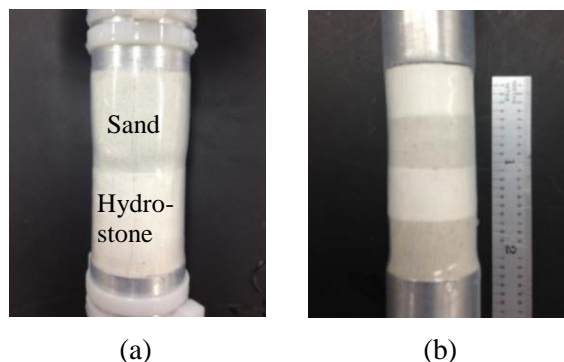


Fig. 2. Illustration of two types of samples used (a) two-layer sample (b) four-layer sample.

3. NUMERICAL SIMULATION

3.1. Sample Assembly Generation

Numerical models are developed to simulate the triaxial testing and measure the mechanical properties of layered samples for which laboratory testing is impractical. Particle Flow Code 3D (PFC3D), which is developed based on the discrete element method [12], is used for numerical simulation in this study. It is designed primarily to model the mechanical behavior of an assembly of rigid spherical particles.

In PFC3D, stiff rocks such as sandstone are modeled by bonding every particle to its neighbors and the resulting assemblage is regarded as solid. The variation in the bond type, stiffness, and strength, which corresponds to the effect of cement, together with the micro-properties of particles enables us to model materials with different macroscopic mechanical properties [10, 13].

In order to simulate triaxial testing in PFC3D, models which can represent experimental samples should be generated prior to simulation. Sample preparation involves two steps: sample generation and micro-parameters determination. The main parameters that need to be considered in specimen generation include sample dimension, porosity, and particle size distribution. In the present study, a method of particle generation by radius expansion is employed [13]. The diameter and height of the modeled sample in PFC3D is 25.4 mm and 50.8 mm, respectively. The model contains 15,102 particles, the diameter of which varies between 0.5 mm and 0.75 mm.

3.2. Model Calibration

Before simulating the triaxial testing using PFC3D, numerical micro-properties that best represent the behavior of the rock of interest need to be determined. In this study, numerical micro-properties of hydrostone and sand are determined by following the steps that are described in the literature [10, 14, 15]. The numerical micro-properties of hydrostone include friction coefficient (μ), normal stiffness (k_n), shear stiffness (k_s), parallel bond normal stiffness (k_{np}), parallel bond shear stiffness (k_{sp}), parallel bond normal strength (σ_p), parallel bond shear strength (τ_p), and parallel bond radius multiplier (λ_p). The numerical micro-properties of sand particles include friction coefficient, normal stiffness (k_n), shear stiffness (k_s), and friction coefficient (μ). The calibration process utilizes a trial-and-error approach to determine the microscopic parameters of particles and bonds that produce reasonable macroscopic behavior of hydrostone and sand which are obtained from the experimental testing. Table 2 and 3 show the numerical micro-property parameters for hydrostone and sand, respectively.

Table 2. Micro-properties for hydrostone matrix in PFC3D

Particle properties	
Modulus, E_c (GPa)	32
Normal/Shear Stiffness Ratio, k_n/k_s	3.5
Min. Particle Diameter, D_{min} (mm)	0.5
Max./Min. Diameter Ratio, D_{max}/D_{min}	1.5
Friction Coefficient, μ	0.56
Density, ρ (kg/m ³)	2650
Parallel bond properties	
Modulus, E_p (GPa)	4.1
Normal/Shear Stiffness Ratio, k_{np}/k_{sp}	3.5
Normal Strength, σ_p (MPa)	40
Shear Strength, τ_p (MPa)	40
Radius Multiplier, λ_p	0.85

Table 3. Micro-properties for sand particles in PFC3D

Particle properties	
Modulus, E_c (GPa)	2.1
Normal/Shear Stiffness Ratio, k_n/k_s	3.5
Min. Particle Diameter, D_{min} (mm)	0.5
Max./Min. Diameter Ratio, D_{max}/D_{min}	1.5
Friction Coefficient, μ	1.5
Density, ρ (kg/m ³)	2650

Based on the micro-properties in Table 2 and 3, the mechanical behaviors of hydrostone and sand are determined. The comparison between experimental and numerical results for hydrostone and sand in macroscopic mechanical properties are shown in Table 4 and 5, respectively.

Table 4. Comparison of macroscopic mechanical properties between experimental and numerical results for hydrostone

Properties	Experiment	PFC3D
E (GPa)	6.2	6.4
UCS (MPa)	40.2	40
μ_i	0.564	0.562
ν	0.28	0.31

Table 5. Comparison of macroscopic mechanical properties between experimental and numerical results for sand

Properties	Experiment	PFC3D
E (GPa)	0.363	0.35
μ_i	0.79	0.82

3.3. Layered Sample Setup

In order to examine the contributions of layer properties, such as number, thickness, and strength, on the average strength of a layered reservoir, samples are generated with alternating stiff layers and soft layers. As mentioned in section 2, only two types of layered samples are utilized in the experiments due to the

difficulty in sample preparation, which limits the experimental investigation of layering effect in detail. In the PFC3D simulations, three types of samples are generated, representing different volume ratio between stiff rock layers and soft rock layers (Fig. 3). In each group, four different samples with various numbers of layers and layer thickness are presented, in which the effect of the number of layers and layer thickness on the mechanical properties of layered samples can be investigated in detail.

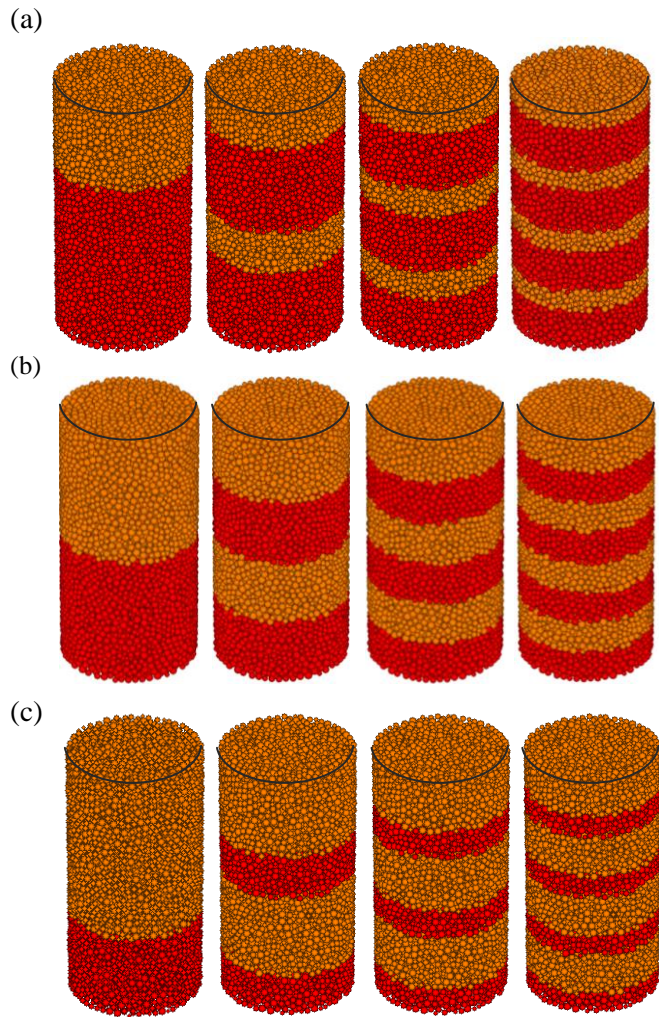


Fig. 3. Illustration of layered reservoir-analog models (a) volume ratio between stiff rocks and soft rocks is 0.5; (b) volume ratio between stiff rocks and soft rocks is 1; (c) volume ratio between stiff rocks and soft rocks is 2.

The diameter of layered samples in PFC3D is 25.4 mm (1 inch) and the height is 50.8 mm (2 inch) for all cases. As illustrated in Fig. 3, brown particles represent stiff layers (hydrostone layers) and red particles compose soft layers (sand layers). The interface between sand layers and hydrostone layers is set to be frictional with a friction coefficient of 0.56.

To investigate the effect of the presence of layers on mechanical properties of layered samples, a set of triaxial testing simulations was performed for samples (Fig. 3) at a confining stress of 2.07 MPa (300 psi). As discussed in section 2, the stiffness of layered rocks can be evaluated based on the axial stress–strain curves. By comparing the stiffness and peak differential stress (peak axial stress minus confining pressure) of layered samples, the influence of layering effect on the average stiffness and strength of layered rocks can be examined.

4. RESULTS AND DISCUSSION

4.1. Influence of the Number of Layers

To investigate the effect of the number of layers and layer thickness on the strength of layered rocks, a set of simulations is performed for samples with two, four, six, and eight layers. In this study, the peak differential stress at the confining pressure of 2.07 MPa is utilized to evaluate the strength of layered rocks. Fig. 4(a) shows the peak differential stress for different number of layers when the volume ratio between stiff rocks and soft rocks is 0.5. Results show that the peak differential stress increases as the number of layers increases from two layers to six layers and remains constant after six layers. As illustrated in Fig. 4(b) and Fig. 4(c), similar conclusions can be drawn for cases where volume ratio between stiff rocks and soft rocks is 1 and 2.

Among all the simulations, the cases which contain more layers in the layered reservoir-analog models in PFC3D are more comparable to the layered reservoir, in which the ratio between layer thickness and layer lateral dimension is small. However, the number of layer in the model cannot be infinitely large because the layer thickness is restricted by the particle size. According to the simulation results, the peak differential stress of layered samples becomes constant when the number of layer exceeds some threshold (six layers when the volume ratio between stiff rocks and soft rocks is 0.5). As a result, the number of layers as well as the layer thickness does not have an effect on the average strength of layered reservoirs, which can be estimated by the value of the peak differential stress at the plateau.

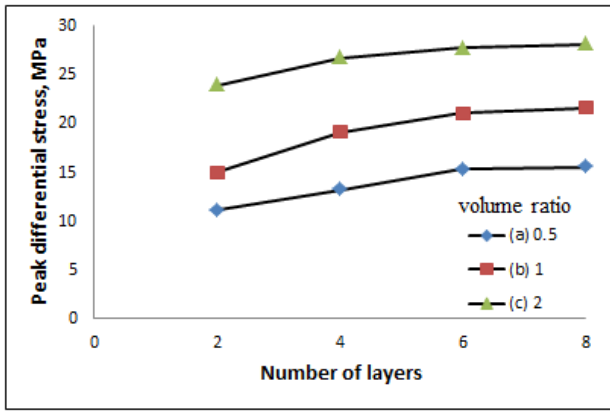


Fig. 4. Peak differential stress with respect to the number of layers at the confining stress of 2.07 MPa (300 psi) with different volume ratios between stiff rocks and soft rocks: (a) 0.5; (b) 1; (c) 2.

4.2. Influence of Bedding Plane Strength

The strength of layered rocks might be also affected by bedding plane strength, which is indicated as interfacial friction coefficient in this study. In order to evaluate the influence of bedding plane strength, the study performed triaxial testing on samples with two different interfacial friction coefficients (0 and 0.56). As shown in Fig. 5, the peak differential stress for friction coefficient of 0 is smaller than the value for friction coefficient of 0.56. This might be because higher friction coefficient at the bedding interface generates higher resistance of layer sliding, causing samples more difficult to fail and resulting in higher rock strength. However the difference between the peak differential stresses at the plateau is quite small compared to the value of the peak differential stress. The reason why the effect of friction coefficient on the layered rock strength is small may be due to the fact that confining stresses on samples are applied by rigid walls in PFC3D simulations, in which layers are confined and not able to slide freely.

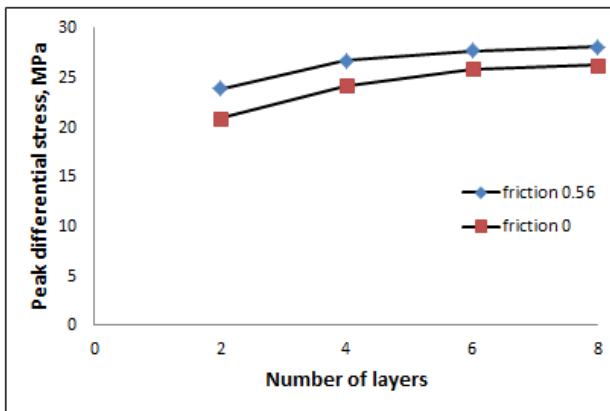


Fig. 5. Peak differential stress with respect to the number of layers with friction coefficient of 0.56 and 0 (the volume ratio between stiff rocks and soft rocks is 2).

4.3. Influence of Volume Ratio

As discussed in section 4.1, the effect of the number of layers, as well as layer thickness, does not have an effect on the overall strength of layered reservoirs. However, according to the simulation results, the strength of layered reservoirs can be indicated by the peak differential stress at the plateau and will change significantly with volume ratio between stiff rocks and soft rocks.

Fig. 6 shows the relationship between the peak differential stress at the plateau of layered reservoir-analog samples and hydrostone volume fraction. The results indicate that the strength of layered reservoir increases as the volume fraction of stiff rocks increases. In particular, the peak differential stress of layered rocks is almost linearly dependent on hydrostone (stiff rocks) volume fraction.

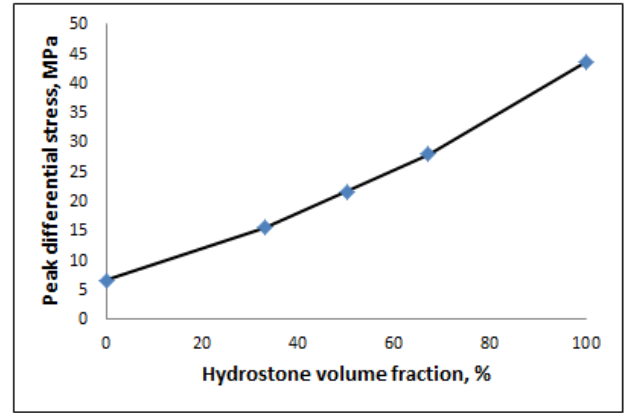


Fig. 6. Peak differential stress of layered rocks with respect to hydrostone volume fraction.

Stiffness is also important to evaluate for fracture height containment [3]. Simulation results in PFC3D show that Young's modulus of layered reservoir-analog models does not depend on the number of layers or layer thickness. However, Young's modulus of hydrostone/sand layered samples in PFC3D is dependent on the volume fraction of hydrostone. For a laminated composite material, the analytical transverse stiffness is given by [16]

$$\frac{1}{E_c} = \frac{V_1}{E_1} + \frac{V_2}{E_2} \quad (3)$$

where E_c is the harmonic Young's modulus, V_1 is the volume fraction of material 1, V_2 is the volume fraction of material 2, E_1 is the Young's modulus of material 1, and E_2 is the Young's modulus of material 2. Fig. 7 shows the comparison between the analytical solution and the numerical solution of Young's modulus for

layered rocks based on hydrostone volume fraction. The results indicate that Young's modulus of layered rocks increases with the volume ratio of stiff rocks.

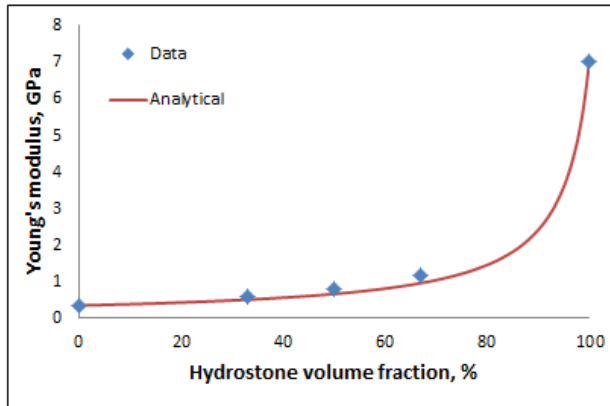


Fig. 7. Comparison between analytical solution and numerical results for Young's modulus at different hydrostone (stiff rocks) volume fraction.

Based on the results illustrated in Fig. 6 and Fig. 7, the strength of rocks can be estimated if the stiffness of the layered rocks is known. Fig. 8 shows that the stiffness-strength relation obtained for the reservoir-analog materials from PFC3D simulations has a similar form to those were obtained from natural rock types [17]. In general, the strength of layered rocks increases as the stiffness increases and the value can be predicted based on the strength-stiffness relation.

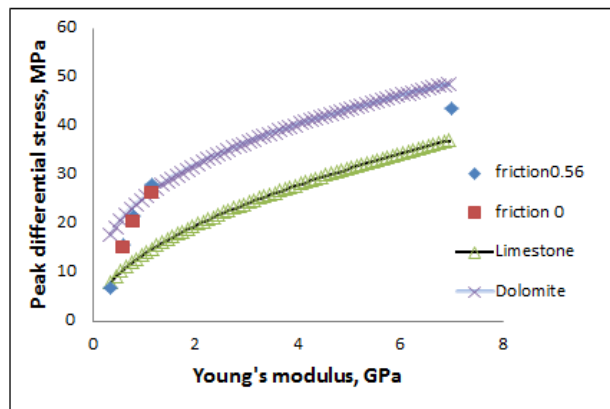


Fig. 8. Comparison between the peak differential stress (obtained at 2.07 GPa confining stress) stiffness relation obtained from the PFC simulations and a UCS-stiffness relation from the literature [17].

5. CONCLUSIONS

In this study, triaxial experimental testing and discrete element analysis using PFC3D are utilized to investigate the layering effect on the overall strength and stiffness of layered reservoir. The results in this study show that the stiffness and strength of a layered sequence are not

affected by factors such bedding plane strength, the number of layers, or layer thickness, whereas they are influenced by the volume fraction of stiff and soft layers. Moreover, the predicted stiffness-strength relation of layered reservoir-analog is in similar form those in the literature for real rocks, from which the strength of layered rocks can be predicted if the stiffness is known.

The results based on this work will contribute to the evaluation of hydraulic fracture height containment. The mechanical property contrast between adjacent layers is considered to be an important mechanism for hydraulic fracture height containment [3, 5, 18]. Based on this study, the stiffness and strength of stratified rock stacks can be determined. As a result, hydraulic fracture height containment within a stratified rock stack can be better evaluated by comparing the contrast of stiffness and strength between adjacent rock stacks.

ACKNOWLEDGMENTS

We would like to acknowledge the industrial associates of the Fracture Research and Application Consortium (FRAC) of the University of Texas at Austin for supporting this work.

REFERENCES

1. Ferrill, D.A., R.N. McGinnis, A.P. Morris, and M.A. Evans. 2014. Control of mechanical stratigraphy on bed restricted jointing and normal faulting: Eagle Ford formation, south central Texas. *AAPG Bulletin* 98, 11: 2477–2506.
2. Fisher, K., and N. Warpinski. 2011. Hydraulic fracture height growth: real data. In *Proceedings of the SPE Annual Technical Conference and Exhibition, Denver, 30 October–2 November 2011*, SPE 145949.
3. Gu, H., and E. Siebrits. 2008. Effect of formation modulus contrast on hydraulic fracture height containment. *SPE Production and Operations* 23, 2: 170–176.
4. Abbas, S., E. Gordeliy, A. Peirce, B. Lecampion, D. Chuprakov, and R. Prioul. 2014. Limited height growth and reduced opening of hydraulic fractures due to fracture offsets: an XFEM Application. In *Proceedings of the SPE Hydraulic Fracturing Technology Conference, Woodlands, Texas, 4–6 February*, SPE 168622.
5. Simonson, E.R., A.S. Abou-Sayed, and R.J. Clifton. 1978. Containment of massive hydraulic fractures. *SPE Journal* 18, 1: 27–32.
6. Zhang, X., R.G. Jeffrey, and M. Thiercelin. 2007. Deflection and propagation of fluid-driven fractures at frictional bedding interfaces: a numerical investigation. *Journal of Structural Geology* 29, 3: 396–410.

7. Warpinski, N.R., R.A. Schmidt, and D.A. Northrop. 1982. In situ stresses: the predominant influence on hydraulic fracture containment. *Journal of Petroleum Technology* 34, 3: 653–664.
8. Teufel, L.M., and J.A. Clark 1984. Hydraulic fracture propagation in layered rock: experimental studies of fracture containment. *SPE Journal* 24, 1: 19–32.
9. Curry, M., T. Maloney, R. Woodruff, and R. Leonard. 2010. Less sand may not be enough. In *Proceeding of the SPE Unconventional Gas Conference, Pittsburgh, Pennsylvania, USA, 23–25 February 2010*, SPE 131783.
10. ITASCA, 2008. *Manual for PFC3D*.
11. Bahorich, B.L. 2012. Examining the effect of cemented natural fractures on hydraulic fracture propagation in hydrostone block experiments, *Master thesis, The University of Texas at Austin, Austin, TX*.
12. Cundall, P.A., and O.D. Strack. 1979. A discrete numerical model for granular assemblies, *Géotechnique* 29, 1: 47–65.
13. Manchanda, R. 2011. Mechanical, failure and flow properties of sands: micro-mechanical models. *Master thesis, The University of Texas at Austin, Austin, TX*.
14. Park, N. 2006. Discrete element modeling of rock fracture behavior: fracture toughness and time-dependent fracture growth, *Ph.D. Thesis, The University of Texas at Austin, Austin, TX*.
15. Potyondy, D.O., and P.A. Cundall. 2004. A bonded-particle model for rock. *International Journal of Rock Mechanics and Mining Sciences* 41, 8: 1329–1364.
16. Jones, R.M. 1975. *Mechanics of Composite Materials*, New York: Hemisphere Publishing Corporation.
17. Zoback, M.D. 2007. *Reservoir Geomechanics*. New York: Cambridge University Press.
18. Van Eekelen, H.A.M. 1982. Hydraulic fracture geometry: fracture containment in layered formation. *SPE Journal* 22, 3: 341–349.